Title: Horizontal transmission and recombination maintain forever young bacterial symbiont genomes

Authors: Shelbi L. Russell[1,2*], Evan Pepper-Tunick[2,3], Jesper Svedberg[2,3], Ashley Byrne[1], Jennie Ruelas Castillo[1], Christopher Vollmers[2,3], Roxanne A. Beinart[4], and Russ Corbett-Detig[2,3*]

Affiliations:

[1.] Department of Molecular Cellular and Developmental Biology. University of California Santa Cruz. Santa Cruz, California, United States of America.

[2.] Department of Biomolecular Engineering. University of California Santa Cruz. Santa Cruz, California, United States of America.

[3.] Genomics Institute, University of California, Santa Cruz, California, United States of America.

[4.] Graduate School of Oceanography. University of Rhode Island. Narragansett, Rhode Island, United States of America.

*To whom correspondence should be addressed: Email: shelbilrussell@gmail.com, russcd@gmail.com

Abstract

Bacterial symbionts bring a wealth of functions to the associations they participate in, but by doing so, they endanger the genes and genomes underlying these abilities. When bacterial symbionts become obligately associated with their hosts, their genomes are thought to decay towards an organelle-like fate due to decreased homologous recombination and inefficient selection. However, numerous associations exist that counter these expectations, especially in marine environments, possibly due to ongoing horizontal gene flow. Despite extensive theoretical treatment, no empirical study thus far has connected these underlying population genetic processes with long-term evolutionary outcomes. By sampling marine chemosynthetic bacterial-bivalve endosymbioses that range from primarily vertical to strictly horizontal transmission, we tested this canonical theory. We found that transmission mode strongly predicts homologous recombination rates, and that exceedingly low recombination rates are associated with moderate genome degradation in the marine symbionts with nearly strict vertical transmission. Nonetheless, even the most degraded marine endosymbiont genomes are occasionally horizontally transmitted and are much larger than their terrestrial insect symbiont counterparts. Therefore, horizontal transmission and recombination enable efficient natural selection to maintain intermediate symbiont genome sizes and substantial functional genetic variation.

Author summary

Symbiotic associations between bacteria and eukaryotes are ubiquitous in nature and have contributed to the evolution of radically novel phenotypes and niches for the involved partners. New metabolic or physiological capacities that arise in these associations are typically encoded by the bacterial symbiont genomes. However, the association itself endangers the retention of bacterial genomic coding capacity. Endosymbiont genome evolution theory predicts that when bacterial symbionts become restricted to host tissues, their populations cannot remove deleterious mutations efficiently. This ultimately results in their genomes degrading to small, function-poor states, reminiscent of organellar genomes. However, many ancient marine endosymbionts do not fit this prediction, but instead retain relatively large, gene-rich genomes, indicating that the evolutionary dynamics of this process need more thorough characterization. Here we show that on-going symbiont gene flow via horizontal transmission between bivalve hosts and recombination among divergent gammaproteobacterial symbiont lineages are sufficient to maintain large and dynamic bacterial symbiont genomes. These findings indicate that many obligately associated symbiont genomes may not be as isolated from one another as previously assumed and are not on a one way path to degradation.

Short title: Forever young bacterial symbiont genomes

Introduction

Bacterial genomes encode an enormous diversity of functions, which enable them to create radically novel phenotypes when they associate with eukaryotic hosts. However, they are at risk of genome degradation and function loss within these associations. Among the diversity of eukaryotic hosts they inhabit, symbiont genome sizes range from nearly unreduced genomes that are similar to their free-living relatives (~3-5 Mb) to highly reduced genomes that are less than 10% of the size of their free-living ancestors (~0.2-0.6 Mb) [1,2]. The degradation process often leaves genes required for the bacterium's role in the symbiosis, and removes seemingly vital genes, such as those involved in DNA repair and replication [1]. Although genome erosion may be enabled in some cases due to "streamlining" benefits [3], it is clear that the process can become problematic and result in symbiont replacement or supplementation [1,4] to accomplish the full repertoire of functions needed in the combined organism. Thus, to fully understand how symbioses evolve, we must first understand the pressures their genomes experience.

Symbiont genome evolution theory predicts that upon host restriction, bacterial genomes begin the steady and inexorable process of decay due to decreased population sizes and homologous recombination rates, which result in inefficacious natural selection [5]. The transmission bottleneck that occurs when symbionts are passed on to host offspring further exacerbates these dynamics by making deleterious mutations more likely to drift to fixation in the next generation [5,6]. Indeed, many endosymbiont taxa exhibit weak purifying selection at the gene level [7–10]. In the early stages of bacterial symbiont-host associations, deleterious mutations arise on each symbiont chromosome and a portion drift or hitch-hike with adaptive mutations to fixation. Subsequently, pseudogenes are lost entirely via deletion [5]. Ultimately, this process is thought to result in an organelle-like genome that is a fraction of the size of its

free-living ancestors and has relegated many of its core cellular functions (*e.g.*, DNA replication and repair, cell wall synthesis, etc.) to the host or lost them entirely.

While the degraded genomes of many endosymbionts are consistent with this theory, such as symbionts of terrestrial sap and xylem-feeding insects [1], a diversity of associations present discrepancies. In particular, most known marine obligate endosymbionts' genomes are at least one megabase in size and contain diverse coding content [11–17], although reduced representatives have recently been found [18]. Large symbiont genomes in obligate associations are usually interpreted as reflecting the earliest stages of genome degradation [19,20], which is surprising considering the antiquity of these associations (*e.g.*, [21,22]). Furthermore, even the vertically transmitted marine symbionts whose phylogenies mirror those of their hosts have only partially degraded genomes [23]. While important genes have been lost in some lineages, such as the recombination and repair gene *recA* and transversion mismatch-repair gene *mutY* [24], their loss did not portend an organelle-like fate.

Symbioses in marine environments exhibit significantly more horizontal transmission between hosts than those in terrestrial environments [25], suggesting that symbiont gene flow between hosts may prevent genome decay by enabling high rates of homologous recombination, efficient natural selection, and the maintenance of highly diverse genome contents. This hypothesis has so far not been tested and it is not known whether marine endosymbionts represent the early stages of genome degradation, as implied by the canonical endosymbiont genome theory, or if on-going gene flow and recombination can stall such genome decay over evolutionary time. Furthermore, although the general process of symbiont genome degradation is well-understood in theory (*e.g.*, [1,2,26]), no empirical study has directly evaluated the role of

horizontal transmission and recombination in facilitating efficient natural selection and, thereby, the suppression of degradation. Interspecific-population level comparisons are essential for testing these important and long-standing questions [26].

To determine which evolutionary forces prevent marine endosymbiont genomes from degrading despite host restriction, we leveraged both population and comparative genomics of six marine bacterial-animal symbioses from three host taxa that exhibit modes of transmission across the spectrum from strict horizontal transmission (*Bathymodiolus* mytilid mussels) [27–29], to mixed mode transmission (solemyid bivalves) [15,30–32], to nearly strict vertical transmission (vesicomyid clams) [23,33–35] (see Fig. 1A-B and S1-S3 Tables). Each of these three groups evolved independently to obligately host either a single intracellular gammaproteobacterial symbiont 16S rRNA phylotype within their gill cells or two or more phylotypes, in the case of some mussels [36,37]. These symbionts provide chemosynthetic carbon fixation, either through sulfide or methane-oxidation, to nutritionally support the association [25]. Hosts are nearly completely dependent on symbiont metabolism [38], and the solemyids have lost the majority of their digestive tracts in response [39]. These associations appear to be obligate for the symbionts as well as the hosts because either the symbionts have never been found living independently, *e.g.*, solemyid [31] and vesicomyid symbionts [40], or they have only been found in the host and surrounding environment, *e.g.*, bathymodiolin symbionts [27,41,42]. Both the vesicomyids and solemyids transmit symbionts to their offspring through allocating tens to hundreds of symbiont cells to their broadcast spawned oocytes [31,33]. While the mechanism of horizontal, host-to-host transfer has not been identified in the *Bathymodiolus* or solemyid symbionts, signatures of rampant horizontal transmission are

evident in the population genetics of both of these groups [15,27,28] and the developmental biology of *Bathymodiolus* [29].

This group of marine symbioses presents an ideal system in which to test the impact of transmission mode and homologous recombination rate on bacterial symbiont genome evolution. The wealth of information known about how the vesicomyid, solemyid, and bathymodiolin symbioses function and evolve makes this a powerful evolutionary model. Furthermore, the similarity of these associations to other invertebrate-bacterial associations in the marine environment, *e.g.*, in mode of reproduction (broadcast spawning), phylogeny (Mollusca-Gammaproteobacteria), immunology (innate), ancestral feeding type (filter or deposit feeders), symbiosis function (nutritional)), makes this an ideal microcosm for understanding how symbiont population genetics impact the process of symbiont genome degradation. Here, we use this model study system and a powerful population genomic approach (described in S1 Fig and S1-S3 Supporting Text), to show that homologous recombination is ongoing even in the most strictly vertically transmitted associations and may enable the maintenance of large and intermediate genome sizes indefinitely.

Results and Discussion

Comparative analyses of host mitochondrial and endosymbiont genome genealogies show strong evidence for horizontal transmission in all six populations (Fig. 1C). Despite this apparent similarity in transmission mode, the vesicomyid endosymbiont genomes are approximately one half the size of the solemyid or mytilid endosymbiont genomes, which themselves are approximately consistent with their free-living ancestors. Nonetheless, at 1-1.2

Mb, the partially degraded vesicomyid endosymbiont genomes are still ten times larger than the smallest terrestrial endosymbionts [1]. The genealogical discordance shown in Figure 1C indicates that horizontal transmission has occurred in the histories of these populations, however, it does not suggest how much because concordance is eroded even by exceedingly low rates of horizontal transmission [43], saturating the signal genealogies can provide. Thus, a finer scaled exploration of symbiont genetic diversity was necessary to characterize the population-level processes influencing genome erosion.

Homologous recombination is an important driver of genetic diversity in many bacterial populations [44,45], and could impact host-associated symbiont populations if diverse genotypes co-occur due to horizontal transmission. Novel genotypes are necessary because recombination among clonal strains, *e.g.*, within a host-restricted clonal population of vertically transmitted endosymbionts, has little impact on haplotypic diversity [46]. To explore the opportunity for recombination among divergent clades of chemosynthetic symbionts, we partitioned symbiont genetic variation to between and within-host variation (*e.g.*, Fig. 2A and S4-S5 Tables). Within vesicomyid symbionts, genetic diversity is strongly subdivided by hosts, and nearly all variation distinguishes host populations (Fig. 2B). Conversely, for mytilid and solemyid endosymbionts, hosts have little impact, and two endosymbionts within a host are almost as divergent as two from different hosts (Fig. 2B).

The distribution of genetic diversity within a single host is even more striking than the pattern between hosts. Within host individuals, *Bathymodiolus* endosymbionts are exceptionally genetically diverse and the allele frequency spectra are qualitatively similar to expectations for an equilibrium neutrally-evolving population (Fig. 2C left and S2 Fig.), consistent with the high

genetic diversities reported for other bathymodiolin symbionts [47]. Conversely, solemyid endosymbionts maintain intermediate and more variable within-host genetic diversity, consistent with a mixture of vertical and horizontal transmission (Fig. 2C middle and S3 Fig.). Finally, vesicomyid endosymbiont populations within hosts are virtually devoid of genetic variability (Fig. 2C right and S4 Fig.). Therefore, despite their literal encapsulation within host cells, mytilid and solemyid symbionts have abundant opportunities to recombine and create fitter chromosomes whereas vesicomyid symbionts must only rarely encounter genetically differentiated individuals.

Although opportunities are limited for vesicomyid endosymbionts, even relatively infrequent homologous recombination events might drive patterns of genome evolution. We therefore developed a theoretical framework of symbiont evolution during mixed transmission modes. Importantly, our model demonstrates that in some conditions these populations can be approximated using a standard Kingman-coalescent and that horizontal transmission is mechanisticanistically linked to observable recombination events between genetically diverse symbiont genomes (S2 Supporting Text and S5-S6 Figs). We then performed extensive coalescent simulations and used a Random Forest-based regression framework to estimate the effective recombination rates for each population (estimated as the population-scaled recombination rate (rho) per site (l); see S6 Table and Materials and Methods). Although our model is clearly an approximation, the results are generally consistent with our prior expectations. The resulting estimated recombination rates are substantially higher in mytilid and solemyid symbionts than in vesicomyid symbionts (Fig. 2D and S4 and S7 Tables), indicating that the potential for recombination within hosts is realized in these species. In fact, these populations have some of the largest effective recombination rates ever reported for

bacteria [48,49]. Nonetheless, we also found evidence for modest rates of recombination within both partially degenerate vesicomyid genomes, despite the loss of many requisite genes in the *Calyptogena magnifica* symbiont [24,50]. For all three symbiont taxa, recombination has a larger impact on genome evolution than mutation (estimated by rho*l/theta in S4 Table), in part due to the relatively low estimates of theta in the symbiont populations. Thus, these bacterial symbionts comprise what might be described as quasi-sexual, rather than clonal, populations.

A fundamental consequence of decreased homologous recombination rates for endosymbionts is that selected mutations cannot be shuffled to form higher fitness chromosomes and remain linked to neutral mutations for longer times. Ultimately, this competition among selected mutations on different haplotypes, termed clonal interference, can drive the fixation of deleterious mutations and reshape genealogies towards long terminal branches and excesses of rare alleles [51] (illustrated in Fig. 3A). Similarly, even in the absence of competition among selected haplotypes, recently completed selected sweeps can reshape linked neutral genealogies if recombination is infrequent [52]. Consistent with this theory, we find abundant rare alleles in the vesicomyid symbiont genomes (Fig. 3 and S4 Table; Tajima's D = -1.98 and -2.03 for *C. magnifica* and *Calyptogena fausta*, respectively), but little skew in the allele frequencies of other endosymbiont populations (D ranges from 0.196 to -1.01). Importantly, it is unlikely that differences in host species demography have driven these differences, *e.g.,* recent population expansions specifically in vesicomyid clams. In fact, we found less allele frequency skew in the mitochondrial genomes than in the vesicomyid symbionts for all species considered, and the strongest negative skew in the allele frequencies in the mitochondrial genome of *B. septemdierum* from the Lau Basin (D = -1.9, S4 Table). Additionally, relative rates of molecular evolution between symbiont populations follow the expected trend, with

dN/dS values of 0.14, 0.096, 0.083 for vesicomyid, solemyid and bathymodiolin genomes, respectively (pairwise Wilcoxon test p-values: bathymodiolin-vesicomyid p=4.60e-14, solemyid-vesicomyid p= 1.02e-11, and bathymodiolin-solemyid p= 0.0365), consistent with recombination enabling more efficacious purifying selection for sustained periods of time.

Genome structure stasis is thought to be another hallmark of canonical endosymbiont genome evolution, and many terrestrial endosymbioses have reported static, degenerate genomes [1]. Whole genome alignments reveal that the vesicomyid symbiont genomes are highly syntenic, with few rearrangements, insertions, or deletions; whereas the other symbiont genomes are far more structurally dynamic (Fig. 4 and S7 Fig.). Given the role of recombination in altering bacterial genome structure ([50]; Fig. 4A) and the signal of linked selected sites in the vesicomyid symbionts (Fig. 3), recombinational processes may partially underlie genome erosion. This could proceed in the following way: first, a rare recombination event induces a deletion that drifts to high frequency in the within-host population. With homologous recombination events occurring so rarely in these endosymbiont genomes, natural selection would be unable to efficiently purge deleterious deletions. Although, inversions, which can be highly mutagenic by inverting the translated strand, inducing replication-transcription machinery collisions [53], are nearly absent potentially due to their high fitness costs. If symbionts with chromosomes bearing the recombination-induced deletion are exclusively transmitted to offspring during vertical transmission, then the deletion would be fixed in all subsequent symbionts in that host lineage. Multiple instances of this process would incrementally reduce the size of the symbiont genome.

In contrast, the solemyid symbiont genomes exhibit increasing degrees of structural dynamics with increasing divergence time. Highly divergent solemyid symbionts, such as the *S. velum* and *S. pervernicosa* symbionts, exhibit genomes that are as structurally dynamic as strictly horizontally transmitted associations (Fig. 4B vs C). However, over shorter time scales, such as the duration of time since the *S. velum* and *S. elarraichensis* symbionts diverged (discussed below), structural changes appear to be dominated by insertions and deletions (indels; confirmed for 30 Kb segments of the *S. elarrachensis* symbiont draft genome in S7 Fig.). Rapidly evolving indels have also been reported at the species level for *S. velum* [15]. Potentially underlying indel dynamics, we found that the solemyid symbionts have far more mobile genetic elements than any of the other symbiont genomes (S8 Table). High mobile element content is consistent with a combination of environmentally-exposed and host-associated periods [54], and mirrors the early stages of symbiosis [19,20], as well as the early stages of eukaryotic asexuality [55]. The mobile elements exhibit homology to different environmental bacteria, implying many independent insertion events (S9 Table).

It is plausible that vesicomyid symbionts' horizontal transmission and recombination rates are at the beginning of the range of values that permit genome decay. Our data indicates that they undergo horizontal transmission (Figs. 1C) and recombine (Fig. 2D and S4 Table). Furthermore, signatures of genetic variation consistent with linked selection and sustained intermediate genome sizes indicate that selection is sufficiently efficacious to maintain some functional diversity in these populations, counter to the expectations for the original theory on endosymbiont genome evolution [5,6]. While the fossil record and previous phylogenetic analyses indicate that the vesicomyid symbionts and clades of solemyid symbionts have been

in continuous host association for long periods of time [21,22,56], and thus genome erosion has been prevented, precise divergence dates are needed to confirm this conclusion.

Divergence date estimates for hosts and symbionts indicate that the observed patterns in symbiont genome structure have been maintained over many millions of years (Fig. 5, S8 Fig., and S10-12 Tables). Similar to prior work [21], we estimated that the vesicomyid bivalves evolved from their non-symbiotic ancestors around 73 million years ago (mya) (95% highest posterior density (HPD) = 62.59 - 76.70 my; Fig. 5B). We estimated a similar divergence date for the vesicomyids' monophyletic symbionts of around 84 my (95% CI = 42.37 - 165.09 my; Fig. 5A), which is remarkable given that their loss of DNA repair genes and reduced selection efficacy has likely increased their substitution rate (and may have been accounted for by using a relaxed local molecular clock). Interestingly, the clade of gammaproteobacteria that contains the vesicomyid symbionts, termed the SUP05 clade, also contains the thiotrophic *Bathymodiolus* symbionts and free-living bacteria with genomes in the range of 1.17-1.71 Mb (Fig. 5A), from which the vesicomyid symbionts are approximately 220 my (95% CI = 127 - 381my) diverged. This indicates that the vesicomyid symbiont genomes have eroded 58% at most, depending on the symbiont lineage and the ancestral state. Thus, over tens of millions of years of host association, the vesicomyid symbiont genomes have exhibited high degrees of stasis and have only degraded moderately (*e.g.*, in vesicomyid symbionts with 1 Mb vs. 1.2 Mb genomes).

The solemyids present a similar, but more complicated situation, likely owing to their antiquity, as the hosts first appeared in the fossil record more than 400 mya [22], when the ocean basins had much different connectivity [57]. While host-switching and novel symbiont acquisition have

certainly occurred in Solemyidae, and our data indicates such an event may have happened after *S. velum* and *S. pervernicosa* diverged (Fig. 5A), it may be relatively rare across geological time. Whole genome mitochondrial and symbiont phylogenies indicate that the North Atlantic *Solemya* species *S. velum* and *S. elarraichensis* are sisters that diverged around 129 mya (95% HPD = 124 - 152 my; Fig. 5B), and their symbionts likely co-speciated with them around the same time (170 mya, 95% CI = 89 - 325 my; Fig. 5A). Divergence and subsequent speciation may have been due to the opening of the Atlantic, which occurred contemporaneously (180-200 mya; [58]). Thus, the vertically transmitted *S. velum* and *S. elarriachensis* symbionts have maintained genomes similar in size to their free-living relatives over hundreds of millions of years of host association.

Given the extreme ages of the solemyid and vesicomyid associations, our data suggest that moderate rates of recombination have allowed their symbiont genomes to maintain functional diversity characteristic of a free-living or moderately reduced genome, respectively. Evidence from the insect endosymbionts experiencing extreme genome size reduction indicates that genome erosion is possible over time frames as short as 5-20 my (*e.g.*, [59–66]). Thus, ample time has passed for these symbiont genomes to erode, but horizontal transmission and recombination have likely prevented it.

Conclusion

Here we empirically show that symbiont genome sizes and functional diversity are predicted by the rate of gene flow into and among symbiont populations via horizontal transmission and homologous recombination. Although we have only investigated three independently evolved associations, we see this system serving as a microcosm for marine associations more

generally, as many other associations exhibit similar biologies (*e.g.*, intracellular, autotrophic, broadcast-spawning, etc. [36]) and all are governed by the same population genetic principles. Amazingly, we found that symbiont gene flow between hosts is ongoing in one of the most intimate marine associations, the vertically transmitted vesicomyids. These results suggest that there is a range of possible intermediate genome degradation states that can be maintained over millions of years with sufficient recombination. Therefore, symbiont genome evolution following host restriction is not a one-way, inescapable process that ends in an organelle-like state as it is commonly presented [2,5,6]. These results validate long-standing but untested theory and suggest that the diversity of symbioses found to exhibit intermediate rates of horizontal transmission and incomplete genome degradation may be undergoing similar population-level processes.

Materials and Methods

1. Samples and Genomic Data Production

Sample collection

We obtained chemosynthetic bivalve samples from hydrothermal vents, cold seeps, and reducing coastal sediments from around the world (S1 Table). *Calyptogena magnifica* samples were collected from the East Pacific Rise (EPR) hydrothermal vent fields between 1998 and 2004. *Calyptogena fausta* were collected from the Juan de Fuca (JDF) Ridge hydrothermal vent system in 2004. The single *Calyptogena extenta* specimen was collected from Monterey Canyon in 1995. *Solemya pervernicosa* samples were obtained from the Santa Monica sewage outfall in 1992 (as in [15]). *Solemya velum* were collected from Point Judith, RI, as described in [15]. *B. childressi* were sampled from the Veatch Canyon cold seep off of New England. *B.*

septemdierum was sampled from the ABE and Tu'i Malila hydrothermal vent sites in Lau Basin. All tissue samples were stored at -80°C until sterile dissection or subsection of previously sterile-dissected gill tissue as described in [15].

DNA extraction and Illumina sequencing

We extracted DNA from gill samples for each host individual sampled using Qiagen DNeasy kits and otherwise following the manufacturer's instructions. We quantified DNA concentrations using a qubit dsDNA kit and normalized each sample to 10 ng/ul for Illumina library preparations. We produced the majority of our Illumina sequencing libraries for each sample using a Tn5-based protocol for tagmentation followed by dual-indexing PCR using HiFi DNA polymerase (Kappa Bioscience) and custom primer sequences (IDT) designed to uniquely label both i5 and i7 indexes for each sample (Tn5 enzyme was expressed and purified in-house). Indexed samples were pooled and sequenced on single lanes of a Hiseq4000. We sequenced a total of four lanes of Hiseq4000 paired-end 150 bp sequencing across the entire study. Additionally, we obtained a subset of samples for *C. magnifica* using genomic methods from our previous work ([15], S1 Table). We also used a dataset we have previously collected for *S. velum*, specifically the population from Point Judith, Rhode Island ([15], S1 Table). The specific library preparation methods and number of read pairs obtained for each sample included in this work are listed in S1 Table.

Nanopore sequencing

For each *de novo* genome assembly in this work, we selected a representative from each host population based on DNA quality as determined using genomic tapestation and DNA concentration based on qubit readings. We sequenced each sample on a single minion flow cell

using the ligation-based 1D chemistry, SQK-LSK109 kit per ONT instructions with minor adjustments. The end-repair reaction was incubated for 30 minutes each at 20℃ and 65℃ and the ligation reaction was performed for 30 minutes instead of the recommended 10 minutes. Read counts obtained and mean read lengths are available in S1 Table. We performed basecalling using the Albacore basecaller v2.0.1 and we discarded the subset of reads whose mean quality score was less than 7. These are the set marked nominally as “failed” by the basecaller software.

De novo symbiont genome assembly

Reference genomes for the *B. septemdierum*, *B. childressi*, *S. pervernicosa,* and *C. fausta* symbionts were assembled using combined Nanopore and Illumina reads. First, we assembled the Nanopore reads using the long read assembly program wtdbg2 [67] using the “ont” presets option and setting the parameter -k to 15. Then, we performed two rounds of reference genome improvement by aligning Illumina sequencing reads from the same individual to the resulting unfiltered assembly and polishing the Pilon software package [68]. We used BWA-MEM [69] to align Illumina reads in each subsequent polishing round.

We assembled the *C. extenta* symbiont genome from an Illumina library prepared for the single sampled individual using IDBA [70] and SPAdes [71]. While both assemblies were highly contiguous (N50=596007 and 604961 bp, respectively), the SPAdes assembly was able to merge two contigs that were split in the IDBA assembly, so the two contig SPAdes assembly was used for downstream analyses. Comparisons of synteny demonstrated that this join was found in other Vesicomyid endosymbiont genomes suggesting it is correct (see below).

Because read mixtures include both host genomic DNA, mitochondrial DNA, and genomic DNA from other bacterial species, we then rigorously filtered the resulting contigs to extract only high confidence contigs contributed by bacteria of the study species. To identify symbiont contigs, we called ORFs with Prodigal v2.60 [72] and annotated coding sequences with BLAST [73] as described in [15] (NCBI nr, TrEMBL, and UniProt database accessed on April 7, 2019). We annotated ribosomal RNAs with RNAmmer [74] and transfer RNAs with tRNAscan [75]. Using the taxonomic information encoded in the annotation, we identified contigs that were confidently of symbiont origin. Then, using these contigs, we filtered the remaining contigs by GC content, read coverage, and coding density using custom scripts. Finally, we evaluated the quality of the assemblies with CheckM [76] and by testing for the presence of core bacterial phylogenetic markers [77] (see S2 Table).

Host mitochondrial genome assembly

Mitochondrial genomes were assembled from Nanopore reads, which were subsequently corrected with Illumina data, as described above, or they were assembled from Illumina reads directly. As the different samples contained different mitochondrial coverage, higher short read coverage was often better than lower long read coverage for recovering these genomes. We assembled mitochondrial genomes for *C. fausta and B. septemdierum* with IDBA [70] using Illumina data from two of the highest depth-of-coverage samples (*C. fausta* 31 and *B. septemdierum* 231, respectively). The complexity of the *B. septemdierum* data prevented IDBA from finishing within a week, so we first removed low coverage nuclear kmers (<10x) with Quake [78]. The *C. extenta* mitochondrial genome was assembled along with the symbiont genome using SPAdes [71], as described above. We were able to use the Nanopore-based assembly from *Bathymodiolus childressi* from New England for the mitochondrial genome.

Lastly, the complete mitochondrial genome for *S. pervernicosa* was available from [15], so we did not reassemble it here.

After assembly, we identified the mitochondrial scaffold by blasting the full set of scaffolds against a database containing the currently available set of 19 bivalve mitochondrial genomes. Then, we annotated the mitochondrial genome with MITOS [79]. For mitochondrial genomes lacking conserved genes, we repeated genome assembly and mitochondrial genome identification and annotation with a different sample to verify we obtained the full sequence. See S1 Supporting Text for a description of the species identification verification process.

Short read alignment

After producing endosymbiont genome assemblies and host mitochondrial genome assemblies for each host/endosymbiont species, we aligned short read Illumina data from each individual to a reference genome consisting of both of these genomes. Genomes assembled previously for the *C. magnifica* symbiont ([11], accession NC_008610.1) and mitochondrian ([80], accession NC_028724.1), and the *S. velum* symbiont ([13] and accession NZ_JRAA00000000.1) and mitochondrian ([81] and accession NC_017612.1) were used as references for these populations. We used the BWA mem software package [69], and we then sorted and removed duplicate reads using the samtools software package [82]. After this, we performed indel realignment for each sample separately using the “IndelRealigner” function within the Genome Analysis Toolkit (GATK) software package [83].

Genotyping and variant filtration for each host individual

We called consensus genotypes for each individual jointly using the GATK “UnifiedGenotyper” option and we ran the program with otherwise default parameters except we required that it output all sites rather than just all variable positions. We filtered variant sites using the vcftools software package [84] largely following the GATK best practices as we have done in our previous work [15]. Briefly, we required that each site have a minimum quality/depth ratio of 2, a maximum Fisher’s strand value of 60, a minimum nominal genotype quality of 20 and a maximum number of reads with mapping quality zero at a putatively variant site of 5. For analyses of within host individual variation for fixation index (Fst) calculations, we also obtained a multiple pileup file using samtools and filtered sites that were not retained after applying these filters. See S1 Supporting Text for an estimate of the consensus genotyping error rate.

Within-host diversity analysis

We called within-host SNP and indel variants for endosymbionts and mitochondria using the method from [85]. Briefly, we created mpileup files from BWA bam alignment files for all individuals from each host species using SAMTools [82]. Then, we called variants and calculated pairwise diversity using the perl script from [85], which only considers sites within one standard deviation of the average genome coverage, filters SNPs around indels, and requires an alternate allele count in excess of the cumulative binomial probability of sequencing error at that site. As very closely related sister taxa have not been sampled for most of these bacterial genomes, ancestral/derived alleles could not be identified and we could not plot unfolded allele frequency spectra. Instead, folded allele frequency spectra were calculated for minor alleles and plotted in R.

No heteroplasmy was detected within the mitochondrial within-host populations (see S4 Table), suggesting that these bivalves do not experience double uniparental mitochondrial inheritance. This is important given our expectations regarding mitochondrial-symbiont co-divergence under strict vertical transmission.

2. Genome Analyses

Population genealogy inference

We produced multiple fasta sequence files for each population for the host mitochondrial genomes and for the concatenated symbiont genomes from the set of filtered consensus genotype calls. We then used the phylogenetic software package RAxML [86] using a GTR+G model and 1,000 bootstrap replicates to estimate the phylogenetic relationships among samples and to quantify uncertainty in our phylogenetic relationships. Using FigTree, we rooted the trees by their midpoints and created cladograms for topological comparisons.

Analysis of polymorphic and recombinant sites

Using the fasta files described above, we filtered sites to only retain biallelic SNPs with a minimum genotype quality of 10. Without indels, these resequenced genomes were already aligned. Then we used the aligned SNP data to calculate Waterson's theta [87], pi [88], and the proportion of pairwise sites where all 4-gametes, *i.e.,* all pairwise combinations of alleles, are represented. We then binned the 4-gamete sites by the distances between alleles, with bins at 1e1, 1e2, 1e3, 1e4, 1e5, and 1e6 bp, for model fitting (described below).

Whole genome structural alignment

We generated whole genome alignment plots by first aligning bacterial genome assemblies with MUMmer 3.23 [89], using the nucmer algorithm and default parameters. In addition to the mb-scale genomes we assembled and referenced above, we obtained mb-scale genomes for *Bathymodiolus septemdierum* str. Myojin knoll ([42], accession GCA_001547755.1), *Bathymodiolus thermophilus* str. EPR9N ([90], accession GCF_003711265.1), and *Vesicomyosicus okutanii* ([12], accession NC_009465.1) from NCBI for alignment. The nucmer output was converted into the BTAB format with the MUMmer tool show-coords and was then visualized using a custom Python script. When necessary, some scaffolds in the bacterial assemblies were split into two parts in order to convert a circular genome into a linear alignment plot.

We used the whole genome aligner progressiveMauve [91] to compare genome synteny on the 10s of Kb scale between the *S. velum* and *S. elarraichensis* symbionts. First, we reordered the contigs comprising the *S. elarraichensis* symbiont draft genome [15] by the *S. velum* symbiont assembly [13] with the reorder contig function in progressiveMauve. Then, we then aligned the *S. velum* symbiont genome pairwise against the *S. elarraichensis* symbiont's reordered contigs and the *S. pervernicosa* symbiont genome we assembled. We plotted the alignment backbone files in the R package genoPlotR [92].

Mobile element analysis

We identified mobile elements in the endosymbiont genome sequences by BLAST. First, we generated BLAST database files with the makeblastdb command from the ACLAME [93] and ICEberg [94] nucleotide and amino acid databases of transposable, viral, and conjugative elements. Next, we used blastp and blastn to compare endosymbiont amino acid sequences

and full genome sequences, respectively, to these databases (cutoff values: minimum alignment length of 50 nucleotides or 50% amino acid query coverage, 90% identity, and e-value 1e-6). Overlapping hits were consolidated into a single mobile element-containing region (SI Appendix Table S9).

Ortholog identification

We identified putative orthologous sequences among sets of bacterial genomes by a reciprocal best blast approach. To do this, we first performed pairwise blasts between each pair of genomes' coding sequences with blastn (-best_hit_overhang 0.1 -best_hit_score_edge 0.1 -evalue 1e-6), alternating each sequence as the query/subject. We parsed these results to only retain the best hits with >50% identity and >100 bp alignment lengths. Then, using a custom perl script, we compared hits between all pairs to identify genes with reciprocal best hits among all taxa each homologous gene was detected in. We used the resulting matrix of these reciprocal best hits to extract the coding sequences for each ortholog for each species from the genome fasta files for downstream analysis.

dN/dS analysis

To evaluate the impact of homologous recombination on patterns of natural selection at the molecular level over long periods of time we computed the average fixation rate among endosymbiont lineages at nonsynonymous and synonymous sites (dN/dS). This ratio of these two values is an approximate measure of the strength of purifying selection under the assumption that most nonsynonymous substitutions are deleterious. For all genes where a single ortholog was found to be shared among all symbiont lineages we began by producing codon aware alignments using MASCE [95]. Then, we compared each orthologous alignment

for pairs of symbiont lineages within each group (solemyid, vesicomyid and bathymodiolin) to estimate dN and dS using the codeml package in the PAML v4.9 framework [96]. We excluded all comparisons for which dS < 0.05 or dS > 2, as values that exceed this range are often thought to yield unreliable estimates of rates of molecular evolution due to low statistical power and saturated substitutions, respectively. We then compared the distributions of dN/dS for each symbiont group comparison using a Wilcoxon test.

Divergence dating

Taxon selection:

To construct dated phylogenies for hosts and symbionts, we downloaded related genomes from NCBI. For the host divergence analysis, all of the bivalve mitochondrial genomes available as of early 2020 and four gastropod mitochondrial genomes were downloaded to serve as ingroups and outgroups, respectively (35 total taxa: 31 bivalves and four gastropods; see S10 Table). For the symbiont divergence analysis, bacterial genomes were identified for inclusion in the analysis by BLAST [73]. While residing in a relatively constrained clade of proteobacteria, these chemosynthetic symbionts do not form a monophyletic clade, have free-living relatives, are basal to more derived groups in Gammaproteobacteria, and are currently taxonomically unclassified, so it was necessary to fish out related genomes by identifying sequence homology. To do this, we aligned the nucleotide coding sequences from each one of the seven symbiont genomes we sequenced and/or analyzed against NCBI's Prokaryotic RefSeq Genomes database with blastn (-best_hit_overhang 0.1 -best_hit_score_edge 0.1 -evalue 1e-6). Based upon the diversity of hits across symbionts and genomes, we selected the top three best hits to each gene as taxa to include in the full genome divergence analysis (59 total taxa: 58 gammaproteobacteria and one alphaproteobacterium; see S11 Table).

Multiple sequence alignment:

As bivalve mitochondrial genomes exhibit notoriously diverse structural arrangements [97], we used the whole rearrangement-aware genome aligner progressiveMauve [91] to align the molluscan mitochondrial genomes. These alignments were manually inspected and converted to fasta format in Geneious Prime (version 11.0.6+10) [98].

We identified and aligned orthologous proteins among these diverse bacterial genomes with bcgTree [99], then we back-translated the resulting amino acid alignments to nucleic acids with RevTrans [100]. As bcgTree only includes protein-coding genes, we manually extracted and aligned 16S and 23S ribosomal RNA sequences for these taxa with Mafft (using the accurate mafft-linsi setting) [101]. Although recombination clearly occurs frequently in the solemyid and mytilid symbiont populations, we decided against removing recombinant sites because doing so may exacerbate recombination-induced artifacts [102]. Finally, we concatenated these alignments with the nucleotide alignments from bgcTree/RevTrans with a custom perl script and inspected them in Geneious Prime.

Phylogenetic inference and divergence dating:

We first inferred maximum likelihood phylogenies with RAxML (version 8.2.1, with parameters: f a -m GTRGAMMA -N 1000) [86] to verify that the taxa selected were able to resolve the relationships among hosts and among symbionts and free-living bacteria. Both mitochondrial and symbiont phylogenies were well-resolved (S8 Fig.).

We inferred Bayesian phylogenies and dated node divergences for host mitochondria in Beast2 [103]. After several rounds of parameter testing to ascertain the speciation model and calibration date distribution that best fit the data (see S1 Supporting Text), we selected the Yule model of speciation, with a gamma distributed Hasegawa, Kishino, and Yano (HKY) model of substitution and a relaxed local molecular clock, and we calibrated dates to the base of the ingroup, Bivalvia. We used the fossil-based minimum appearance date for bivalves of 520 million years (first appearance estimated in Fossilworks [104] from fossil data in [105,106]). MCMC chains were run in duplicate until posterior probability convergence, around 8e8 steps for mitochondria. We also performed independent divergence date estimations in RelTime [107,108] and PATHd8 [109] to compare to the Beast2 results (see S1 Supporting Text and S12 Table).

Given the consistency in RelTime and Beast2 estimates for mitochondria (S12 Table) and the unreasonably long run times necessary (several weeks) for symbiont dated phylogenies to reach posterior convergence in Beast2, we estimated symbiont divergence times in RelTime. We used the previously estimated divergence date for Gammaproteobacteria of 1.89 billion years (based on calibration to the cyanobacterial-caused atmospheric oxygenation event [110]) with a log-normal distribution to calibrate a relaxed local clock, using a gamma-distributed Tamura-Nei model of substitution, allowing for invariant sites. All trees were plotted in FigTree.

Symbiont species descriptions

Using the genomic, phylogenetic, and divergence data we generated above, we diagnosed and described the six symbiont species sequenced in this study. These classifications will be helpful in future investigations and discussions of symbiont function and diversity. Diagnoses of

symbiont genera and descriptions of symbiont species are described in the S3 Supplemental Text and listed in S3 Table.

3. Parameter Estimation via Approximate Bayesian Computation

Simulation Setup

To simultaneously estimate the rates of horizontal transmission, effective homologous recombination rates, and the recombinant tract length, we used an approximate Bayesian computation approach. Here, we define the population-scaled per-base pair recombination rate, rho, to be equal to two times the effective population size times the per-base pair rate of gene conversion (rho=2*N_er). The recombination tract length, l, is defined as the length of the gene conversion segment in base pairs. We used the bacterial sequential Markovian coalescent simulation framework, FastSimBac [111], to simulate neutral coalescence across a range of input parameters (see S2 Supporting Text for model proof). We drew the effective mutation rate from a log-uniform distribution (3e-5,1e-2), the effective recombination rate from a log-uniform (1e-6,1e-2) distribution and the recombinant tract length from a uniform (1,1e5) distribution. Because the clonal frame cannot be inferred for the *Bathymodiolus* and *Solemya* symbiont populations, presumably due to the high levels of recombination relative to other bacteria, we did not supply the program with a fixed precomputed clonal frame for any simulations. In total we performed 100,000 simulations and we used subsets from each simulation to obtain summary statistics to train the variable sample size simulations.

Summary statistics

We selected a set of summary statistics that each incorporate some feature of the overall diversity (relevant for theta), and the overall effective recombination rate per site (rho*l).

Specifically, we computed two estimators of theta, Waterson's theta [87], and pi [88], and we included the proportion of pairs of non-singleton SNPs at various genomic distances where all four possible combinations of alleles are observed in our sample. We placed the divisions between distance bins for pairwise comparisons of sites at 1e1, 1e2, 1e3, 1e4, 1e5, 1e6 base pairs.

Model fitting via random forest regression

We use the scikit-learn package to perform random forest regression to obtain estimates of each parameter for each endosymbiont population, using the 4-gamete sites identified above and a custom Python script available on Github. First, we confirmed that our summary statistics are sufficient to accurately fit our desired population parameters using out-of-bag score during model training and for each population sample size (S6 Table). Although the score is often slightly lower for smaller sample sizes, this approach performs sufficiently well and consistently across samples for our applications here. We additionally obtained confidence intervals for each parameter estimate using the forestsci package [112]. It should be noted that our simulations assume an equilibrium population. If this assumption is violated in a subset of the taxa that we examined, it might affect our parameter estimates. Nonetheless, it is unlikely that the large-scale differences in estimated parameters that we observe among groups, which are consistent with prior expectations, are entirely attributable to this potential bias.

Method validation on existing datasets

In light of the relatively high recombination rates that we estimate, it is valuable to confirm that our approach for estimating rho and theta performs as expected. We therefore applied our method to the *Bacillus cereus* dataset [113] that has been studied in similar contexts using

several related approaches [111,113,114]. In prior work with this dataset, estimates of the total impact of recombination, rho*l/theta, have varied somewhat, from approximately 3.7 [111] to 35.9 [113] and 229 [114]. Using our method, we obtain a value intermediate to these at 17.1, which indicates a moderate impact of recombination on genome evolution. This result suggests that our method is reliable and does not substantially inflate recombination rate estimates.

Read-Backed Phasing to Confirm Recombination Estimates

Because we used consensus symbiont genomes during model fitting, it could be possible that the high estimated rates of recombination in solemyid and bathymodiolin samples are an artefact of differential haplotype coverage across the genomes of genetically diverse symbiont chromosomes. We therefore sought to confirm our recombination rate estimates via comparing the rate of occurrence of all four possible configurations of two proximal alleles using read-backed phasing. Because each read-pair must ultimately derive from a single DNA fragment, when two alleles are observed on the same read or read pair, in the absence of errors, they must reflect an allelic combination that's observed within a single bacterial chromosome.

We therefore analyzed in aggregate all reads that overlapped two or more consensus alleles for each population and computed the fraction of all four possible sampling configurations. More specifically, we computed the proportion of reads sampled from across all reads in all individuals that contained alleles, AB, Ab, aB, and ab, for two adjacent biallelic sites with alleles A/a and B/b. To reduce the impact of sequencing errors, we recorded a site as containing all four possible configurations when all configurations were present at proportion greater than 0.05 in the total set of read pairs. We further limited comparisons to alleles where we could obtain at

least 100 observations of both sites on single read pairs. We excluded the populations of vesicomyid endosymbionts from this analysis because too few polymorphic sites were present within the distances spanned by individual read pairs to confidently infer the frequencies of 4D sites. However, because samples from these populations contain virtually no within-host variation, we have little reason to doubt the accuracy of the consensus genotypes resulting from differential coverage of genetically diverse bacterial haplotypes.

Because we are sampling a much larger number of lineages than we did in analyzing the consensus genome sequences, we would expect if anything is different that we observe higher rates of sites where all four possible allele configurations are present. This is precisely what we found. Specifically, we observe higher proportions of pairs of sites where all four possible allelic combinations are represented at each distance considered and in each population in the read-backed dataset than in the consensus chromosomes (S7 Table). Furthermore, because we have placed conservative cutoffs on the proportions of read pairs required to consider a pair of sites as containing all four alleles these values are likely underestimates of the true rates. Our observed rates of four-gamete test failures is therefore consistent with our analyses of consensus genome sequences and confirms that recombination must be common within these endosymbiont populations.

References:

1. Moran NA, Bennett GM. The Tiniest Tiny Genomes. Annu Rev Microbiol. 2014;68: 195–215. doi:10.1146/annurev-micro-091213-112901
2. Lo W-S, Huang Y-Y, Kuo C-H. Winding paths to simplicity: genome evolution in facultative insect symbionts. Lai E-M, editor. FEMS Microbiol Rev. 2016;40: 855–874. doi:10.1093/femsre/fuw028
3. Giovannoni SJ, Cameron Thrash J, Temperton B. Implications of streamlining theory for microbial ecology. ISME J. 2014;8.
4. Meseguer AS, Manzano-Marín A, Coeur d'Acier A, Clamens A-L, Godefroid M, Jousselin E. *Buchnera* has changed flatmate but the repeated replacement of co-obligate symbionts is not associated with the ecological expansions of their aphid hosts. Mol Ecol. 2017;26: 2363–2378. doi:10.1111/mec.13910
5. McCutcheon JP, Moran NA. Extreme genome reduction in symbiotic bacteria. Nat Rev Microbiol. 2011 [cited 3 Jan 2017]. doi:10.1038/nrmicro2670
6. Toft C, Andersson SGE. Evolutionary microbial genomics: insights into bacterial host adaptation. Nat Rev Genet. 2010;11: 465–475. doi:10.1038/nrg2798
7. Lambert JD, Moran NA. Deleterious mutations destabilize ribosomal RNA in endosymbiotic bacteria. Proc Natl Acad Sci. 1998;95: 4458–4462. doi:10.1073/pnas.95.8.4458
8. Kuwahara H, Takaki Y, Yoshida T, Shimamura S, Takishita K, Reimer JD, et al. Reductive genome evolution in chemoautotrophic intracellular symbionts of deep-sea Calyptogena clams. Extremophiles. 2008;12: 365–374. doi:10.1007/s00792-008-0141-2
9. Herbeck JT, Funk DJ, Degnan PH, Wernegreen JJ. A Conservative Test of Genetic Drift in the Endosymbiotic Bacterium Buchnera: Slightly Deleterious Mutations in the Chaperonin groEL. Genetics. 2003; 10.
10. Shapiro BJ, Alm E. The slow:fast substitution ratio reveals changing patterns of natural selection in γ-proteobacterial genomes. ISME J. 2009;3: 1180–1192. doi:10.1038/ismej.2009.51
11. Newton ILG, Woyke T, Auchtung TA, Dilly GF, Dutton RJ, Fisher MC, et al. The Calyptogena magnifica Chemoautotrophic Symbiont Genome. Science. 2007;315: 998–1000. doi:10.1126/science.1138438
12. Kuwahara H, Yoshida T, Takaki Y, Shimamura S, Nishi S, Harada M, et al. Reduced Genome of the Thioautotrophic Intracellular Symbiont in a Deep-Sea Clam, Calyptogena okutanii. Curr Biol. 2007;17: 881–886. doi:10.1016/j.cub.2007.04.039
13. Dmytrenko O, Russell SL, Loo WT, Fontanez KM, Liao L, Roeselers G, et al. The genome of the intracellular bacterium of the coastal bivalve, *Solemya velum*: a blueprint for thriving in and out of symbiosis. BMC Genomics. 2014;15. doi:doi:10.1186/1471-2164-15-924
14. Miller IJ, Vanee N, Fong SS, Lim-Fong GE, Kwan JC. Lack of Overt Genome Reduction in the Bryostatin-Producing Bryozoan Symbiont "Candidatus Endobugula sertula." Drake HL, editor. Appl Environ Microbiol. 2016;82: 6573–6583. doi:10.1128/AEM.01800-16
15. Russell SL, Corbett-Detig RB, Cavanaugh CM. Mixed transmission modes and dynamic genome evolution in an obligate animal–bacterial symbiosis. ISME J. 2017; 1359–1371. doi:10.1038/ismej.2017.10
16. Hendry TA, Freed LL, Fader D, Fenolio D, Sutton TT, Lopez JV. Ongoing Transposon-Mediated Genome Reduction in the Luminous Bacterial Symbionts of Deep-Sea Ceratioid Anglerfishes. Moran NA, editor. mBio. 2018;9: e01033-18, /mbio/9/3/mBio.01033-18.atom. doi:10.1128/mBio.01033-18
17. Jäckle O, Seah BKB, Tietjen M, Leisch N, Liebeke M, Kleiner M, et al. Chemosynthetic

symbiont with a drastically reduced genome serves as primary energy storage in the marine flatworm *Paracatenula*. Proc Natl Acad Sci. 2019; 201818995. doi:10.1073/pnas.1818995116
18. George EE, Husnik F, Tashyreva D, Prokopchuk G, Horák A, Kwong WK, et al. Highly Reduced Genomes of Protist Endosymbionts Show Evolutionary Convergence. Curr Biol. 2020;30: 925-933.e3. doi:10.1016/j.cub.2019.12.070
19. Ran L, Larsson J, Vigil-Stenman T, Nylander JAA, Ininbergs K, Zheng W-W, et al. Genome Erosion in a Nitrogen-Fixing Vertically Transmitted Endosymbiotic Multicellular Cyanobacterium. Ahmed N, editor. PLoS ONE. 2010;5: e11486. doi:10.1371/journal.pone.0011486
20. Oakeson KF, Gil R, Clayton AL, Dunn DM, von Niederhausern AC, Hamil C, et al. Genome Degeneration and Adaptation in a Nascent Stage of Symbiosis. Genome Biol Evol. 2014;6: 76–93. doi:10.1093/gbe/evt210
21. Johnson SB, Krylova EM, Audzijonyte A, Sahling H, Vrijenhoek RC. Phylogeny and origins of chemosynthetic vesicomyid clams. Syst Biodivers. 2017;15: 346–360. doi:10.1080/14772000.2016.1252438
22. Sharma PP, Zardus JD, Boyle EE, González VL, Jennings RM, McIntyre E, et al. Into the deep: A phylogenetic approach to the bivalve subclass Protobranchia. Mol Phylogenet Evol. 2013;69: 188–204. doi:10.1016/j.ympev.2013.05.018
23. Ozawa G, Shimamura S, Takaki Y, Takishita K, Ikuta T, Barry JP, et al. Ancient occasional host switching of maternally transmitted bacterial symbionts of chemosynthetic vesicomyid clams. Genome Biol Evol. 2017;9: 2226–2236.
24. Kuwahara H, Takaki Y, Shimamura S, Yoshida T, Maeda T, Kunieda T, et al. Loss of genes for DNA recombination and repair in the reductive genome evolution of thioautotrophic symbionts of <i>Calyptogena clams<\i>. BMC Evol Biol. 2011;11: 285.
25. Russell SL. Transmission mode is associated with environment type and taxa across bacteria-eukaryote symbioses: a systematic review and meta-analysis. FEMS Microbiol Lett. 2019; fnz013.
26. Wernegreen JJ. Endosymbiont evolution: predictions from theory and surprises from genomes: Endosymbiont genome evolution. Ann N Y Acad Sci. 2015;1360: 16–35. doi:10.1111/nyas.12740
27. Fontanez KM, Cavanaugh CM. Evidence for horizontal transmission from multilocus phylogeny of deep-sea mussel (Mytilidae) symbionts: Horizontal transmission of mussel symbionts. Environ Microbiol. 2014;16: 3608–3621. doi:10.1111/1462-2920.12379
28. Won Y-J, Hallam SJ, O'Mullan GD, Pan IL, Buck KR, Vrijenhoek RC. Environmental acquisition of thiotrophic endosymbionts by deep-sea mussels of the genus Bathymodiolus. Appl Environ Microbiol. 2003;69: 6785–6792. doi:10.1128/AEM.69.11.6785-6792.2003
29. Wentrup C, Wendeberg A, Huang JY, Borowski C, Dubilier N. Shift from widespread symbiont infection of host tissues to specific colonization of gills in juvenile deep-sea mussels. ISME J. 2013;7: 1244–1247.
30. Gustafson RG, Reid RG. Association of bacteria with larvae of the gutless protobranch bivalve Solemya reidi (Cryptodonta: Solemyidae). Mar Biol. 1988;97: 389–401.
31. Russell SL, McCartney E, Cavanaugh CM. Transmission strategies in a chemosynthetic symbiosis: detection and quantification of symbionts in host tissues and their environment. Proc R Soc B Biol Sci. 2018;285: 9.
32. Krueger DM, Gustafson RG, Cavanaugh CM. Vertical transmission of chemoautotrophic symbionts in the bivalve Solemya velum (Bivalvia: Protobranchia). Biol Bull. 1996;190:

195–202.
33. Ikuta T, Igawa K, Tame A, Kuroiwa T, Kuroiwa H, Aoki Y, et al. Surfing the vegetal pole in a small population: extracellular vertical transmission of an “intracellular” deep-sea clam symbiont. R Soc Open Sci. 2016;3: 160130. doi:10.1098/rsos.160130
34. Cary SC, Giovannoni SJ. Transovarial inheritance of endosymbiotic bacteria in clams inhabiting deep-sea hydrothermal vents and cold seeps. Proc Natl Acad Sci. 1993;90: 5695–5699.
35. Breusing C, Johnson SB, Vrijenhoek RC, Young CR. Host hybridization as a potential mechanism of lateral symbiont transfer in deep-sea vesicomyid clams. Mol Ecol. 2019; mec.15224. doi:10.1111/mec.15224
36. Dubilier N, Bergin C, Lott C. Symbiotic diversity in marine animals: the art of harnessing chemosynthesis. Nat Rev Microbiol. 2008;6: 725–740. doi:10.1038/nrmicro1992
37. Duperron S, Halary S, Lorion J, Sibuet M, Gaill F. Unexpected co-occurrence of six bacterial symbionts in the gills of the cold seep mussel Idas sp. (Bivalvia: Mytilidae). Environ Microbiol. 2008;10: 433–445. doi:10.1111/j.1462-2920.2007.01465.x
38. Noellette Conway, Judith McDowell Capuzzo, Brian Fry. The Role of Endosymbiotic Bacteria in the Nutrition of Solemya velum: Evidence from a Stable Isotope Analysis of Endosymbionts and Host. Limnol Oceanogr. 1989;34: 249–255.
39. Robert G. B. Reid, Frank R. Bernard. Gutless Bivalves. Sci New Ser. 1980;208: 609–610.
40. Decker C, Olu K, Arnaud-Haond S, Duperron S. Physical proximity may promote lateral acquisition of bacterial symbionts in vesicomyid clams. López-García P, editor. PLoS ONE. 2013;8: e64830. doi:10.1371/journal.pone.0064830
41. Ponnudurai R, Kleiner M, Sayavedra L, Petersen JM, Moche M, Otto A, et al. Metabolic and physiological interdependencies in the Bathymodiolus azoricus symbiosis. ISME J. 2016 [cited 3 Jan 2017]. Available: http://www.nature.com/ismej/journal/vaop/ncurrent/full/ismej2016124a.html
42. Ikuta T, Takaki Y, Nagai Y, Shimamura S, Tsuda M, Kawagucci S, et al. Heterogeneous composition of key metabolic gene clusters in a vent mussel symbiont population. ISME J. 2016;10: 990.
43. Brandvain Y, Goodnight C, Wade MJ. Horizontal Transmission Rapidly Erodes Disequilibria Between Organelle and Symbiont Genomes. Genetics. 2011;189: 397–404. doi:10.1534/genetics.111.130906
44. Shapiro BJ, Friedman J, Cordero OX, Preheim SP, Timberlake SC, Szabo G, et al. Population Genomics of Early Events in the Ecological Differentiation of Bacteria. Science. 2012;336: 48–51. doi:10.1126/science.1218198
45. Rosen MJ, Davison M, Bhaya D, Fisher DS. Fine-scale diversity and extensive recombination in a quasisexual bacterial population occupying a broad niche. Science. 2015;348: 1019–1023.
46. Chong RA, Park H, Moran NA. Genome Evolution of the Obligate Endosymbiont Buchnera aphidicola. Agashe D, editor. Mol Biol Evol. 2019;36: 1481–1489. doi:10.1093/molbev/msz082
47. Ansorge R, Romano S, Sayavedra L, Kupczok A, Tegetmeyer HE, Dubilier N, et al. Diversity matters: Deep-sea mussels harbor multiple symbiont strains. bioRxiv. 2019 [cited 24 Jul 2019]. doi:10.1101/531459
48. Vos M, Didelot X. A comparison of homologous recombination rates in bacteria and archaea. ISME J. 2009;3: 199–208. doi:10.1038/ismej.2008.93
49. Lin M, Kussell E. Inferring bacterial recombination rates from large-scale sequencing datasets. Nat Methods. 2019;16: 199–204. doi:10.1038/s41592-018-0293-7

50. Nilsson AI, Koskiniemi S, Eriksson S, Kugelberg E, Hinton JCD, Andersson DI. Bacterial genome size reduction by experimental evolution. Proc Natl Acad Sci U S A. 2005;102: 12112–12116.
51. Neher RA. Genetic Draft, Selective Interference, and Population Genetics of Rapid Adaptation. Annu Rev Ecol Evol Syst. 2013;44: 195–215. doi:10.1146/annurev-ecolsys-110512-135920
52. Smith JM, Haigh J. The hitch-hiking effect of a favourable gene. Genet Res. 1974;23: 23–25.
53. Merrikh CN, Merrikh H. Gene inversion potentiates bacterial evolvability and virulence. Nat Commun. 2018;9: 4662. doi:10.1038/s41467-018-07110-3
54. Newton ILG, Bordenstein SR. Correlations Between Bacterial Ecology and Mobile DNA. Curr Microbiol. 2011;62: 198–208. doi:10.1007/s00284-010-9693-3
55. Glémin S, Galtier N. Genome Evolution in Outcrossing Versus Selfing Versus Asexual Species. In: Anisimova M, editor. Evolutionary Genomics. Totowa, NJ: Humana Press; 2012. pp. 311–335. doi:10.1007/978-1-61779-582-4_11
56. Stewart FJ, Cavanaugh CM. Bacterial endosymbioses in Solemya (Mollusca: Bivalvia)—Model systems for studies of symbiont–host adaptation. Antonie Van Leeuwenhoek. 2006;90: 343–360. doi:10.1007/s10482-006-9086-6
57. Cocks LRM, Torsvik TH. Earth geography from 500 to 400 million years ago: a faunal and palaeomagnetic review. J Geol Soc. 2002;159: 631–644. doi:10.1144/0016-764901-118
58. Biari Y, Klingelhoefer F, Sahabi M, Funck T, Benabdellouahed M, Schnabel M, et al. Opening of the central Atlantic Ocean: Implications for geometric rifting and asymmetric initial seafloor spreading after continental breakup: Opening of the Central Atlantic Ocean. Tectonics. 2017;36: 1129–1150. doi:10.1002/2017TC004596
59. Allen JM, Reed DL, Perotti MA, Braig HR. Evolutionary Relationships of “Candidatus Riesia spp.,” Endosymbiotic Enterobacteriaceae Living within Hematophagous Primate Lice. Appl Environ Microbiol. 2007;73: 1659–1664. doi:10.1128/AEM.01877-06
60. Lefevre C. Endosymbiont Phylogenesis in the Dryophthoridae Weevils: Evidence for Bacterial Replacement. Mol Biol Evol. 2004;21: 965–973. doi:10.1093/molbev/msh063
61. Degnan PH, Lazarus AB, Brock CD, Wernegreen JJ. Host–Symbiont Stability and Fast Evolutionary Rates in an Ant–Bacterium Association: Cospeciation of Camponotus Species and Their Endosymbionts, Candidatus Blochmannia. Johnson K, editor. Syst Biol. 2004;53: 95–110. doi:10.1080/10635150490264842
62. Moran N, Wernegreen J. Lifestyle evolution in symbiotic bacteria: insights from genomics. Trends Ecol Evol. 2000;15: 321–326.
63. Takiya DM, Tran PL, Dietrich CH, Moran NA. Co-cladogenesis spanning three phyla: leafhoppers (Insecta: Hemiptera: Cicadellidae) and their dual bacterial symbionts: CODIVERSIFICATION OF SHARPSHOOTER ENDOSYMBIONTS. Mol Ecol. 2006;15: 4175–4191. doi:10.1111/j.1365-294X.2006.03071.x
64. Thao ML, Moran NA, Abbot P, Brennan EB, Burckhardt DH, Baumann P. Cospeciation of Psyllids and Their Primary Prokaryotic Endosymbionts. Appl Environ Microbiol. 2000;66: 2898–2905. doi:10.1128/AEM.66.7.2898-2905.2000
65. Thao ML, Gullan PJ, Baumann P. Secondary (-Proteobacteria) Endosymbionts Infect the Primary (-Proteobacteria) Endosymbionts of Mealybugs Multiple Times and Coevolve with Their Hosts. Appl Environ Microbiol. 2002;68: 3190–3197. doi:10.1128/AEM.68.7.3190-3197.2002
66. Santos-Garcia D, Vargas-Chavez C, Moya A, Latorre A, Silva FJ. Genome Evolution in the Primary Endosymbiont of Whiteflies Sheds Light on Their Divergence. Genome Biol Evol.

2015;7: 873–888. doi:10.1093/gbe/evv038
67. Ruan J, Li H. Fast and accurate long-read assembly with wtdbg2. Bioinformatics; 2019 Jan. doi:10.1101/530972
68. Walker BJ, Abeel T, Shea T, Priest M, Abouelliel A, Sakthikumar S, et al. Pilon: An Integrated Tool for Comprehensive Microbial Variant Detection and Genome Assembly Improvement. Wang J, editor. PLoS ONE. 2014;9: e112963. doi:10.1371/journal.pone.0112963
69. Li H. Aligning sequence reads, clone sequences and assembly contigs with BWA-MEM. arXiv. 2013; arXiv:1303.3997.
70. Peng Y, Leung HCM, Yiu SM, Chin FYL. IDBA-UD: a de novo assembler for single-cell and metagenomic sequencing data with highly uneven depth. Bioinformatics. 2012;28: 1420–1428. doi:10.1093/bioinformatics/bts174
71. Bankevich A, Nurk S, Antipov D, Gurevich AA, Dvorkin M, Kulikov AS, et al. SPAdes: A New Genome Assembly Algorithm and Its Applications to Single-Cell Sequencing. J Comput Biol. 2012;19: 455–477. doi:10.1089/cmb.2012.0021
72. Hyatt D, LoCascio PF, Hauser LJ, Uberbacher EC. Gene and translation initiation site prediction in metagenomic sequences. Bioinformatics. 2012;28: 2223–2230. doi:10.1093/bioinformatics/bts429
73. Camacho C, Coulouris G, Avagyan V, Ma N, Papadopoulos J, Bealer K, et al. BLAST+: architecture and applications. BMC Bioinformatics. 2009;10: 421. doi:10.1186/1471-2105-10-421
74. Lagesen K, Hallin P, Rodland EA, Staerfeldt H-H, Rognes T, Ussery DW. RNAmmer: consistent and rapid annotation of ribosomal RNA genes. Nucleic Acids Res. 2007;35: 3100–3108. doi:10.1093/nar/gkm160
75. Lowe TM, Eddy SR. tRNAscan-SE: a program for improved detection of transfer RNA genes in genomic sequence. Nucleic Acids Res. 1997;25: 955–964.
76. Parks DH, Imelfort M, Skennerton CT, Hugenholtz P, Tyson GW. CheckM: assessing the quality of microbial genomes recovered from isolates, single cells, and metagenomes. Genome Res. 2015;25: 1043–1055. doi:10.1101/gr.186072.114
77. Wu M, Eisen JA. A simple, fast, and accurate method of phylogenomic inference. Genome Biol. 2008;9: 1.
78. Kelley DR, Schatz MC, Salzberg SL. Quake: quality-aware detection and correction of sequencing errors. Genome Biol. 2010;11: 1.
79. Bernt M, Donath A, Jühling F, Externbrink F, Florentz C, Fritzsch G, et al. MITOS: Improved de novo metazoan mitochondrial genome annotation. Mol Phylogenet Evol. 2013;69: 313–319. doi:10.1016/j.ympev.2012.08.023
80. Liu H, Cai S, Zhang H, Vrijenhoek RC. Complete mitochondrial genome of hydrothermal vent clam *Calyptogena magnifica*. Mitochondrial DNA Part A. 2016;27: 4333–4335. doi:10.3109/19401736.2015.1089488
81. Plazzi F, Ribani A, Passamonti M. The complete mitochondrial genome of Solemya velum (Mollusca: Bivalvia) and its relationships with Conchifera. BMC Genomics. 2013;14: 1.
82. Li H, Handsaker B, Wysoker A, Fennell T, Ruan J, Homer N, et al. The Sequence Alignment/Map format and SAMtools. Bioinformatics. 2009;25: 2078–2079. doi:10.1093/bioinformatics/btp352
83. DePristo MA, Banks E, Poplin R, Garimella KV, Maguire JR, Hartl C, et al. A framework for variation discovery and genotyping using next-generation DNA sequencing data. Nat Genet. 2011;43: 491–498. doi:10.1038/ng.806
84. Danecek P, Auton A, Abecasis G, Albers CA, Banks E, DePristo MA, et al. The variant call

format and VCFtools. Bioinformatics. 2011;27: 2156–2158. doi:10.1093/bioinformatics/btr330
85. Russell SL, Cavanaugh CM. Intrahost Genetic Diversity of Bacterial Symbionts Exhibits Evidence of Mixed Infections and Recombinant Haplotypes. Mol Biol Evol. 2017;34: 2747–2761. doi:10.1093/molbev/msx188
86. Stamatakis A. RAxML version 8: a tool for phylogenetic analysis and post-analysis of large phylogenies. Bioinformatics. 2014;30: 1312–1313.
87. Watterson GA. On the number of segregating sites in genetical models without recombination. Theor Popul Biol. 1975;7: 256–276. doi:10.1016/0040-5809(75)90020-9
88. Nei M, Li W-H. Mathematical model for studying genetic variation in terms of restriction endonucleases. Proc Natl Acad Sci. 1979;76: 5269–5273.
89. Kurtz S, Phillippy A, Delcher AL, Smoot M, Shumway M, Antonescu C, et al. Versatile and open software for comparing large genomes. Genome Biol. 2004;5: 1.
90. Ponnudurai R, Sayavedra L, Kleiner M, Heiden SE, Thürmer A, Felbeck H, et al. Genome sequence of the sulfur-oxidizing Bathymodiolus thermophilus gill endosymbiont. Stand Genomic Sci. 2017;12. doi:10.1186/s40793-017-0266-y
91. Darling AE, Mau B, Perna NT. progressiveMauve: Multiple Genome Alignment with Gene Gain, Loss and Rearrangement. Stajich JE, editor. PLoS ONE. 2010;5: e11147. doi:10.1371/journal.pone.0011147
92. Guy L, Roat Kultima J, Andersson SGE. genoPlotR: comparative gene and genome visualization in R. Bioinformatics. 2010;26: 2334–2335. doi:10.1093/bioinformatics/btq413
93. Leplae R, Lima-Mendez G, Toussaint A. ACLAME: A CLAssification of Mobile genetic Elements, update 2010. Nucleic Acids Res. 2010;38: D57–D61. doi:10.1093/nar/gkp938
94. Bi D, Xu Z, Harrison EM, Tai C, Wei Y, He X, et al. ICEberg: a web-based resource for integrative and conjugative elements found in Bacteria. Nucleic Acids Res. 2012;40: D621–D626. doi:10.1093/nar/gkr846
95. Ranwez V, Harispe S, Delsuc F, Douzery EJP. MACSE: Multiple Alignment of Coding SEquences Accounting for Frameshifts and Stop Codons. Murphy WJ, editor. PLoS ONE. 2011;6: e22594. doi:10.1371/journal.pone.0022594
96. Yang Z. PAML 4: Phylogenetic Analysis by Maximum Likelihood. Mol Biol Evol. 2007;24: 1586–1591. doi:10.1093/molbev/msm088
97. Plazzi F, Puccio G, Passamonti M. Comparative Large-Scale Mitogenomics Evidences Clade-Specific Evolutionary Trends in Mitochondrial DNAs of Bivalvia. Genome Biol Evol. 2016;8: 2544–2564. doi:10.1093/gbe/evw187
98. Kearse M, Moir R, Wilson A, Stones-Havas S, Cheung M, Sturrock S, et al. Geneious Basic: An integrated and extendable desktop software platform for the organization and analysis of sequence data. Bioinformatics. 2012;28: 1647–1649. doi:10.1093/bioinformatics/bts199
99. Ankenbrand MJ, Keller A. bcgTree: automatized phylogenetic tree building from bacterial core genomes. Chain F, editor. Genome. 2016;59: 783–791. doi:10.1139/gen-2015-0175
100. Wernersson R. RevTrans: multiple alignment of coding DNA from aligned amino acid sequences. Nucleic Acids Res. 2003;31: 3537–3539. doi:10.1093/nar/gkg609
101. Katoh K, Standley DM. MAFFT Multiple Sequence Alignment Software Version 7: Improvements in Performance and Usability. Mol Biol Evol. 2013;30: 772–780. doi:10.1093/molbev/mst010
102. Hedge J, Wilson DJ. Bacterial Phylogenetic Reconstruction from Whole Genomes Is Robust to Recombination but Demographic Inference Is Not. Vidaver AK, editor. mBio. 2014;5: e02158-14. doi:10.1128/mBio.02158-14

103. Bouckaert R, Heled J, Kühnert D, Vaughan T, Wu C-H, Xie D, et al. BEAST 2: A Software Platform for Bayesian Evolutionary Analysis. Prlic A, editor. PLoS Comput Biol. 2014;10: e1003537. doi:10.1371/journal.pcbi.1003537
104. Behrensmeyer A, Turner A. Taxonomic occurrences of Bivalvia recorded in the Paleobiology Database. In: Fossilworks [Internet]. 2013. Available: http://fossilworks.org
105. Pojeta J, Runnegar B, Kriz J. Fordilla troyensis Barrande: The Oldest Known Pelecypod. Science. 1973;180: 866–868. doi:10.1126/science.180.4088.866
106. Brasier MD, Hewitt RA, Brasier CJ. On the Late Precambrian–Early Cambrian Hartshill Formation of Warwickshire. Geol Mag. 1978;115: 21–36. doi:10.1017/S0016756800040954
107. Battistuzzi FU, Tao Q, Jones L, Tamura K, Kumar S. RelTime Relaxes the Strict Molecular Clock throughout the Phylogeny. Martin B, editor. Genome Biol Evol. 2018;10: 1631–1636. doi:10.1093/gbe/evy118
108. Tamura K, Tao Q, Kumar S. Theoretical Foundation of the RelTime Method for Estimating Divergence Times from Variable Evolutionary Rates. Russo C, editor. Mol Biol Evol. 2018;35: 1770–1782. doi:10.1093/molbev/msy044
109. Britton T, Anderson CL, Jacquet D, Lundqvist S, Bremer K. Estimating Divergence Times in Large Phylogenetic Trees. Anderson F, editor. Syst Biol. 2007;56: 741–752. doi:10.1080/10635150701613783
110. Sheridan PP, Freeman KH, Brenchley JE. Estimated Minimal Divergence Times of the Major Bacterial and Archaeal Phyla. Geomicrobiol J. 2003;20: 1–14. doi:10.1080/01490450303891
111. De Maio N, Wilson DJ. The Bacterial Sequential Markov Coalescent. Genetics. 2017;206: 333–343. doi:10.1534/genetics.116.198796
112. Polimis K, Rokem A, Hazelton B. Confidence Intervals for Random Forests in Python. J Open Source Softw. 2017;2: 124. doi:10.21105/joss.00124
113. Didelot X, Lawson D, Darling A, Falush D. Inference of Homologous Recombination in Bacteria Using Whole-Genome Sequences. Genetics. 2010;186: 1435–1449. doi:10.1534/genetics.110.120121
114. Ansari MA, Didelot X. Inference of the Properties of the Recombination Process from Whole Bacterial Genomes. Genetics. 2014;196: 253–265. doi:10.1534/genetics.113.157172

Acknowledgements:

We thank two anonymous reviewers and Emma George for their helpful comments on the manuscript. For *Calyptogena* freezer samples collected previously, we thank Colleen Cavanaugh and Peter Girguis. For their assistance in collecting *Bathymodiolus* samples from the Lau Basin and Veatch Canyon, respectively, we thank the crews of the R/V *Falkor* and

ROV *ROPOS* and the R/V *Atlantis* and HOV *Alvin*. We thank Peter Wilton for feedback on the symbiont coalescent model derivation. This work was supported by UC Santa Cruz, Harvard University, the Alfred P. Sloan Foundation (to RCD), and the NIH (R35GM128932 to RCD). Funding for Lau Basin collections was provided by the Schmidt Ocean Institute and NSF (OCE-1819530 to RB), Funding for the Veatch Canyon collection was provided via a UNOLS Early Career Training Cruise Program funded by the NSF (OCE-1641453, OCE-1638805, OCE-1214335, OCE- 1655587, and OCE-1649756) and the ONR (N00014–15-1–2583).

Author Contributions:

SLR, study conception and design, samples, Illumina data production, analysis, and writing; EP, Illumina and Nanopore data production; JS, analysis of genome structures and writing; AB, Nanopore data production; JRC, assistance with sampling; CV, Nanopore data production; RB, samples and intellectual contributions; RCD, study conception and design, Illumina and Nanopore data production, theory, analysis, and writing.

Data Accessibility

Data and genome assemblies generated in this study are available through NCBI BioProject number PRJNA562081. Code written and used in our analyses is available from https://github.com/shelbirussell/ForeverYoungGenomes_Russell-et-al.

Figure 1. Nearly-strictly vertically transmitted chemosynthetic endosymbionts exhibit genome erosion despite ongoing horizontal transmission events in their populations. A) Transmission mode spectrum from strict horizontal transmission to strict vertical transmission, with a diversity

of mixed modes, incorporating both strategies, in between. B) Genome sizes from this and previous studies [11–13,90] reveal consistent patterns of moderate genome erosion among the vesicomyid symbionts, but not the other groups with higher rates of horizontal transmission. C) Mitochondrial and symbiont whole genome genealogies are discordant for all groups, indicating that sufficient amounts of horizontal transmission occur in vertically transmitted vesicomyid populations to erode the association between these cytoplasmic genomes. Maximum likelihood cladograms are midpoint rooted, and nodes below 50% bootstrap support are collapsed. Species are color coded by their symbiont transmission mode as in A).

Figure 2. Horizontal transmission and recombination introduce novel alleles into symbiont populations. A) Model of endosymbiont genotype (pink vs. white) distributions under well-mixed high horizontal transmission rates (top) and differentiated, low horizontal transmission rates. B) Horizontally transmitted mytilid (blue) and mixed mode transmitted solemyid (green) symbionts are well mixed among hosts, whereas the nearly strictly vertically transmitted vesicomyid symbionts (yellow-green) are highly differentiated among hosts. Error bars = 95% confidence intervals from non-parametric bootstrapping. C) Intrahost population folded allele frequency spectra (AFS) are shaped by access to gene flow, which is enabled by horizontal transmission and recombination. D) Recombination rates are significantly higher in the mytilid (blue) and solemyid (green) symbiont genomes compared to the vesicomyid symbiont genomes (yellow-green). Error bars = 95% confidence intervals.

Figure 3. Consequences of access to gene flow via horizontal transmission and recombination on the distribution of symbiont genetic diversity between hosts. A) Diagram showing how beneficial alleles (pink) are linked to deleterious alleles (grey) in populations experiencing strong selection on linked sites versus free recombination, and how these processes are reflected in the underlying population genealogies and allele frequency spectra. B,D) Symbiont genealogies as labeled in C) and E), respectively. C,E) Between host allele frequency spectra (AFS) for each host/symbiont species.

Figure 4. Genome structure is shaped by horizontal transmission and recombination. A) Models of recombination-based structural mutation mechanisms. B-D) Whole genome alignments for B) sulfur-oxidizing mytilid, C) solemyid, and D) vesicomyid symbiont genome assemblies with >1 Mb scaffolds.

Figure 5. Chemosynthetic bacterial symbionts and their bivalve hosts exhibit ancient divergence times. A) Maximum likelihood phylogeny inferred from 108 orthologous protein coding genes and the 16S and 23S rRNA genes (outgroup = Alphaproteobacteria; branch labels = bootstrap support fraction) with RelTime divergence date estimates (node bars = 95% confidence intervals). Host-associated bacteria are listed as symbionts of their host species. Bacterial genome sizes are written to the right of the taxon names in the tip labels to highlight trends in genome size across clades. B) Whole mitochondrial Bayesian phylogeny for bivalves (outgroup=Gastropoda; branch labels = posterior probabilities) with divergence dates co-inferred in Beast2 (node bars = 95% highest posterior densities). In both phylogenies,

members of vesicomyid, solemyid, and bathymodiolin (both thioautotrophic and methanotrophic) associations are colored yellow, green, and blue, respectively, as described in Figure 1.

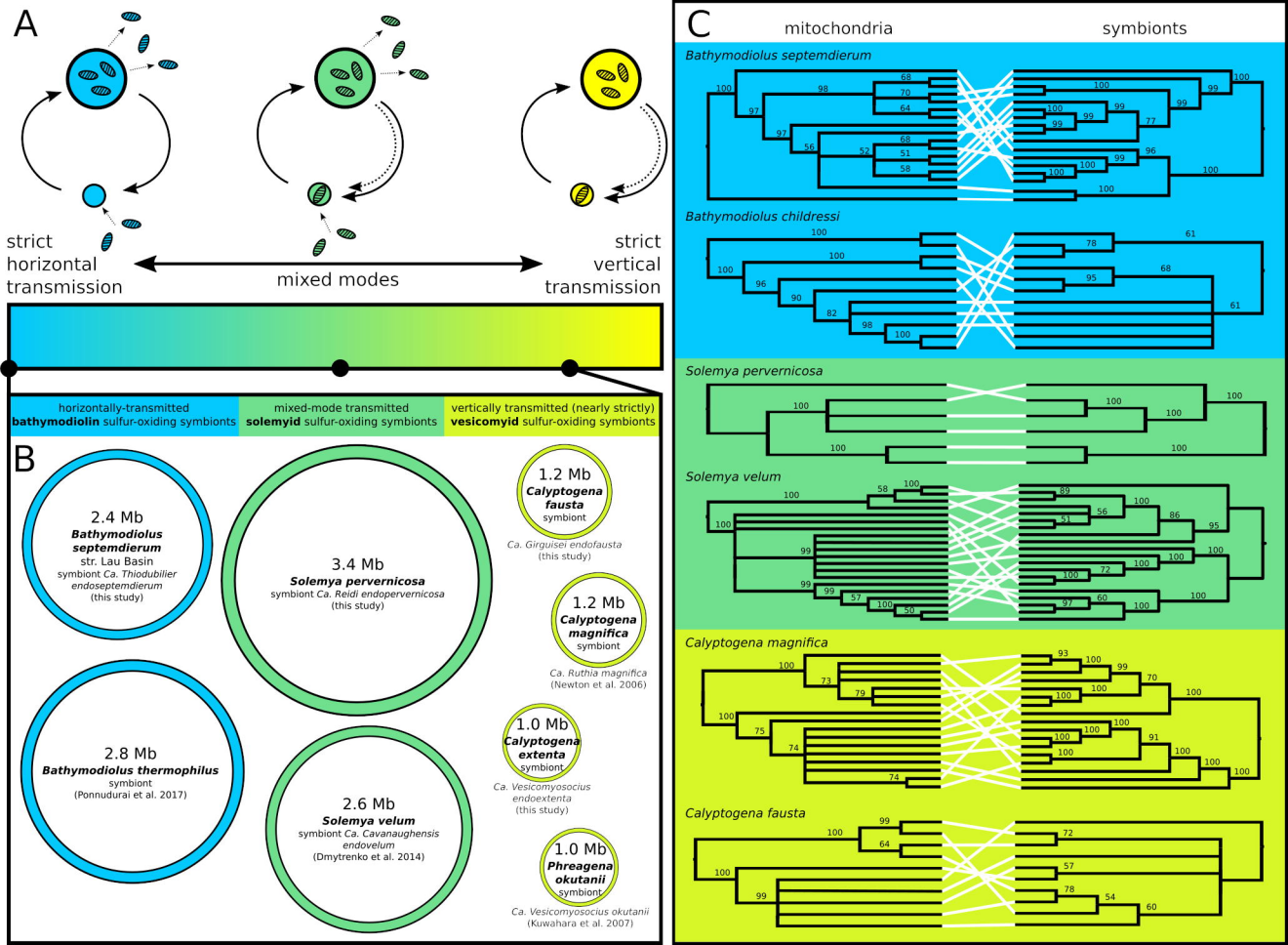
A
strict horizontal transmission
mixed modes
strict vertical transmission
horizontally-transmitted bathymodiolin sulfur-oxiding symbionts
mixed-mode transmitted solemyid sulfur-oxiding symbionts
vertically transmitted (nearly strictly) vesicomyid sulfur-oxiding symbionts
B
2.4 Mb Bathymodiolus septemdierum str. Lau Basin symbiont Ca. Thiodubilier endoseptemdierum (this study)
2.8 Mb Bathymodiolus thermophilus symbiont (Ponnudurai et al. 2017)
3.4 Mb Solemya pervernicosa symbiont Ca. Reidi endopervernicosa (this study)
2.6 Mb Solemya velum symbiont Ca. Cavanaughensis endovelum (Dmytrenko et al. 2014)
1.2 Mb Calyptogena fausta symbiont
Ca. Girguisei endofausta (this study)
1.2 Mb Calyptogena magnifica symbiont
Ca. Ruthia magnifica (Newton et al. 2006)
1.0 Mb Calyptogena extenta symbiont
Ca. Vesicomyosocius endoextenta (this study)
1.0 Mb Phreagena okutanii symbiont
Ca. Vesicomyosocius okutanii (Kuwahara et al. 2007)
C
mitochondria
symbionts
Bathymodiolus septemdierum
Bathymodiolus childressi
Solemya pervernicosa
Solemya velum
Calyptogena magnifica
Calyptogena fausta

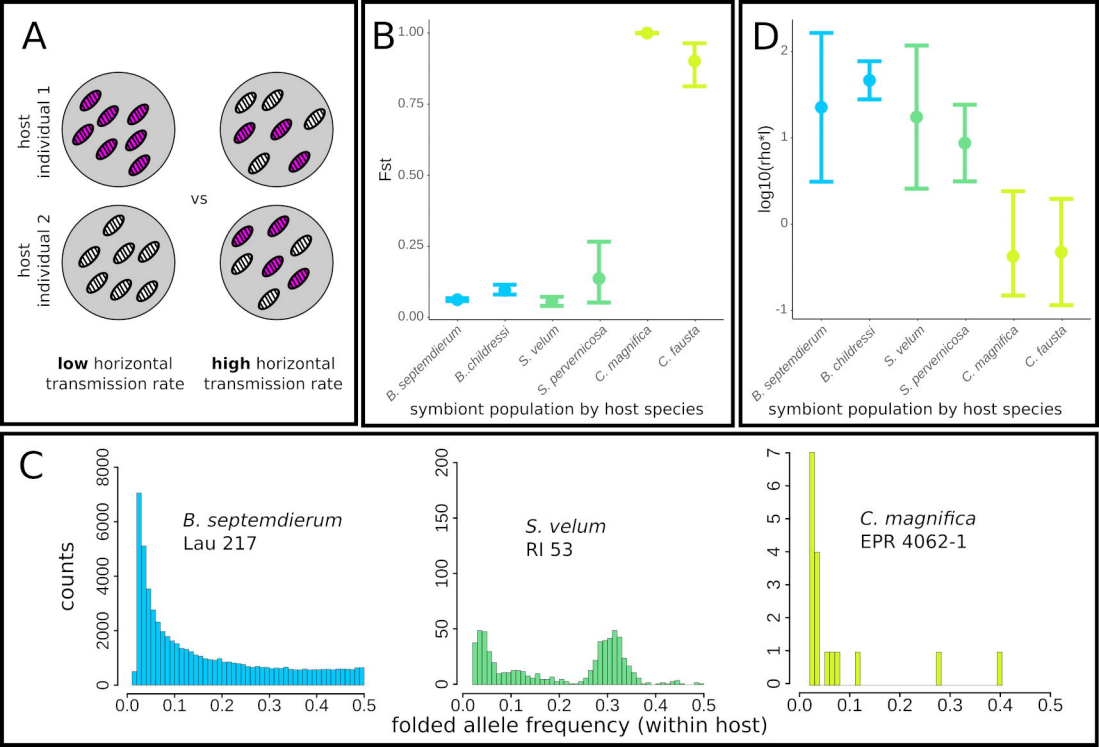
A
host individual 1
host individual 2
vs
low horizontal transmission rate
high horizontal transmission rate
B
Fst
1.00
0.75
0.50
0.25
0.00
B. septemdierum
B. childressi
S. velum
S. pervernicosa
C. magnifica
C. fausta
symbiont population by host species
D
log10(rho*I)
2
1
0
-1
B. septemdierum
B. childressi
S. velum
S. pervernicosa
C. magnifica
C. fausta
symbiont population by host species
C
counts
B. septemdierum
Lau 217
S. velum
RI 53
C. magnifica
EPR 4062-1
0.0
0.1
0.2
0.3
0.4
0.5
folded allele frequency (within host)

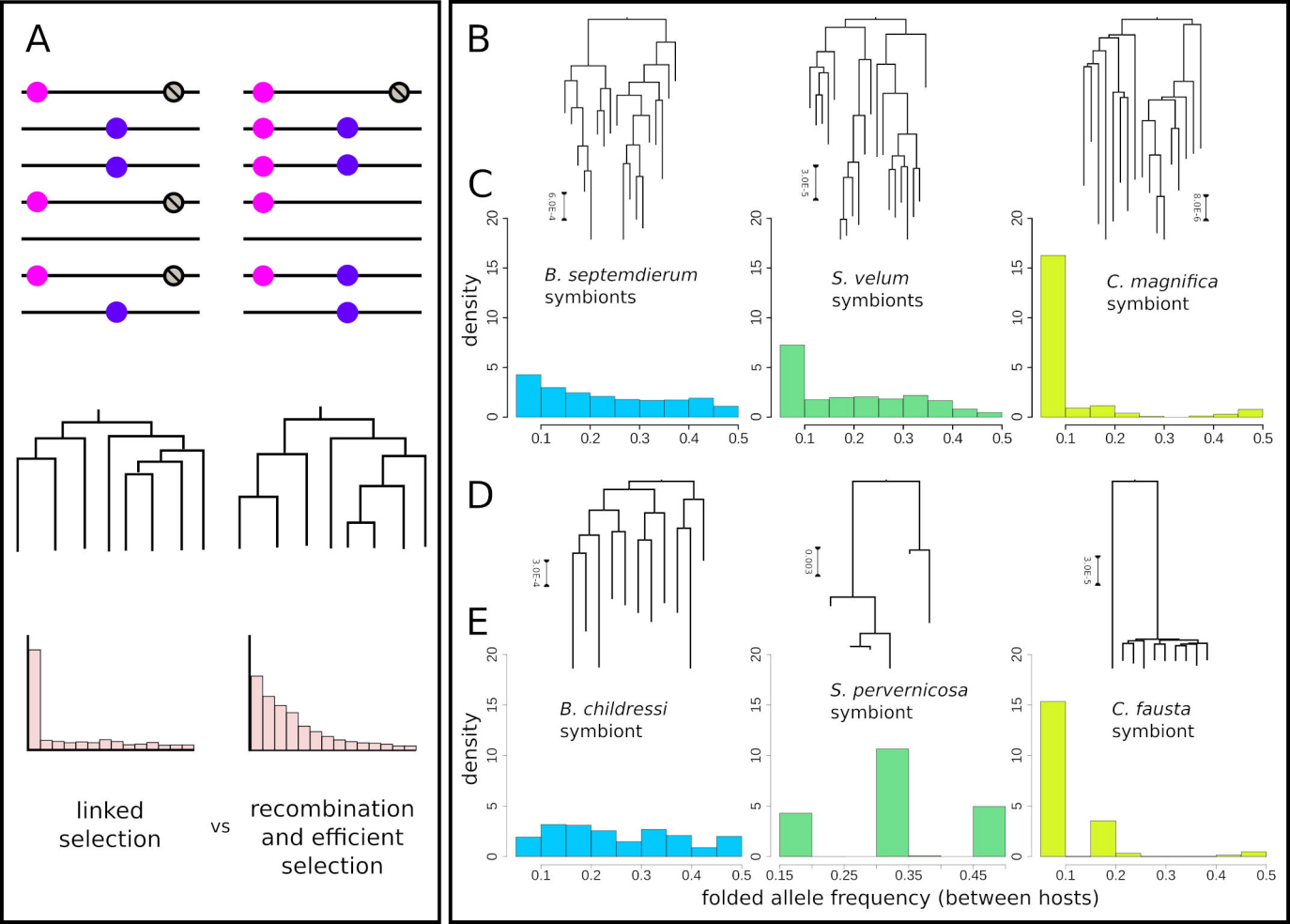
A
linked selection
vs
recombination and efficient selection
B
C
D
E
6.0E-4
3.0E-5
8.0E-6
3.0E-4
0.003
3.0E-5
B. septemdierum symbionts
S. velum symbionts
C. magnifica symbiont
B. childressi symbiont
S. pervernicosa symbiont
C. fausta symbiont
density
folded allele frequency (between hosts)

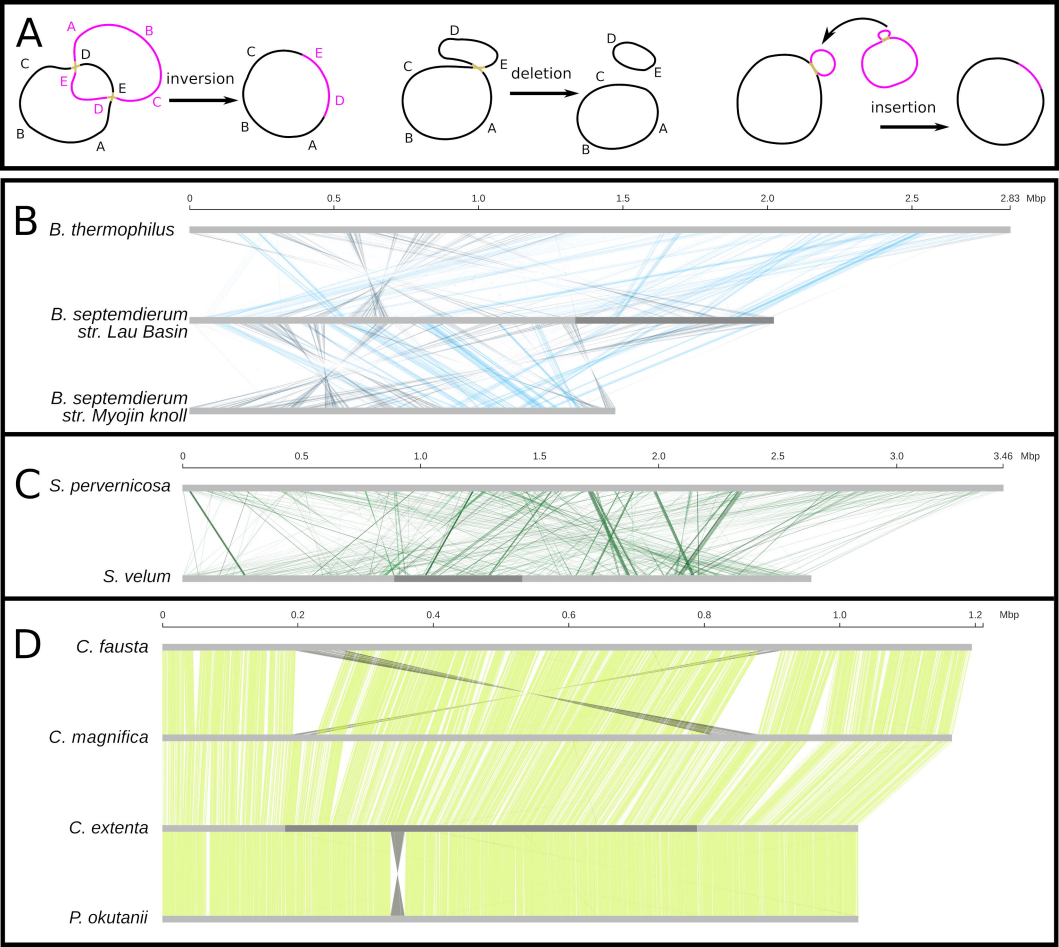
A
inversion
deletion
insertion
B
B. thermophilus
B. septemdierum str. Lau Basin
B. septemdierum str. Myojin knoll
0
0.5
1.0
1.5
2.0
2.5
2.83 Mbp
C
S. pervernicosa
S. velum
0
0.5
1.0
1.5
2.0
2.5
3.0
3.46 Mbp
D
C. fausta
C. magnifica
C. extenta
P. okutanii
0
0.2
0.4
0.6
0.8
1.0
1.2 Mbp

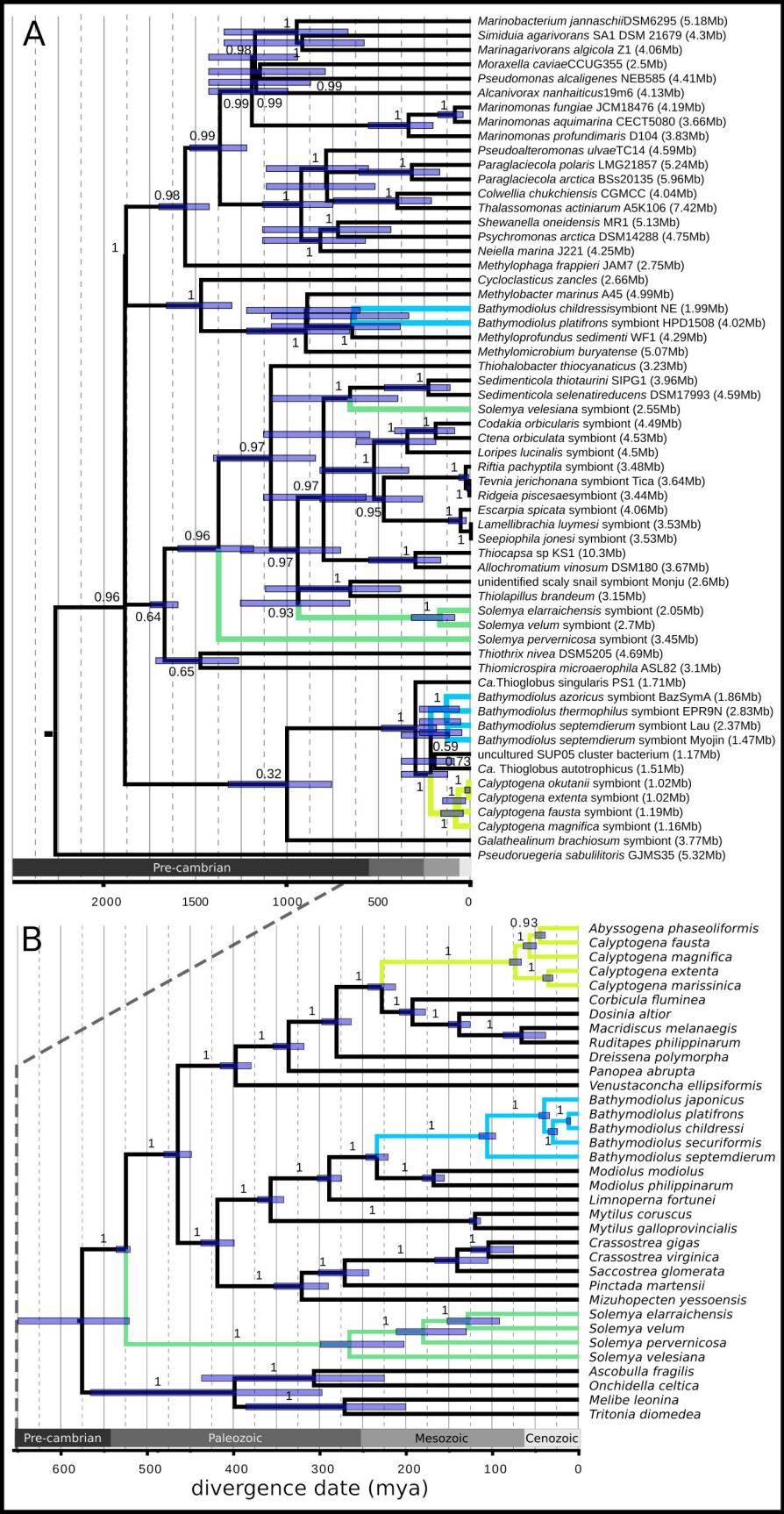
A
Marinobacterium jannaschiiDSM6295 (5.18Mb)
Simiduia agarivorans SA1 DSM 21679 (4.3Mb)
Marinagarivorans algicola Z1 (4.06Mb)
Moraxella caviaeCCUG355 (2.5Mb)
Pseudomonas alcaligenes NEB585 (4.41Mb)
Alcanivorax nanhaiticus19m6 (4.13Mb)
Marinomonas fungiae JCM18476 (4.19Mb)
Marinomonas aquimarina CECT5080 (3.66Mb)
Marinomonas profundimaris D104 (3.83Mb)
Pseudoalteromonas ulvaeTC14 (4.59Mb)
Paraglaciecola polaris LMG21857 (5.24Mb)
Paraglaciecola arctica BSs20135 (5.96Mb)
Colwellia chukchiensis CGMCC (4.04Mb)
Thalassomonas actiniarum A5K106 (7.42Mb)
Shewanella oneidensis MR1 (5.13Mb)
Psychromonas arctica DSM14288 (4.75Mb)
Neiella marina J221 (4.25Mb)
Methylophaga frappieri JAM7 (2.75Mb)
Cycloclasticus zancles (2.66Mb)
Methylobacter marinus A45 (4.99Mb)
Bathymodiolus childressisymbiont NE (1.99Mb)
Bathymodiolus platifrons symbiont HPD1508 (4.02Mb)
Methyloprofundus sedimenti WF1 (4.29Mb)
Methylomicrobium buryatense (5.07Mb)
Thiohalobacter thiocyanaticus (3.23Mb)
Sedimenticola thiotaurini SIPG1 (3.96Mb)
Sedimenticola selenatireducens DSM17993 (4.59Mb)
Solemya velesiana symbiont (2.55Mb)
Codakia orbicularis symbiont (4.49Mb)
Ctena orbiculata symbiont (4.53Mb)
Loripes lucinalis symbiont (4.5Mb)
Riftia pachyptila symbiont (3.48Mb)
Tevnia jerichonana symbiont Tica (3.64Mb)
Ridgeia piscesaesymbiont (3.44Mb)
Escarpia spicata symbiont (4.06Mb)
Lamellibrachia luymesi symbiont (3.53Mb)
Seepiophila jonesi symbiont (3.53Mb)
Thiocapsa sp KS1 (10.3Mb)
Allochromatium vinosum DSM180 (3.67Mb)
unidentified scaly snail symbiont Monju (2.6Mb)
Thiolapillus brandeum (3.15Mb)
Solemya elarraichensis symbiont (2.05Mb)
Solemya velum symbiont (2.7Mb)
Solemya pervernicosa symbiont (3.45Mb)
Thiothrix nivea DSM5205 (4.69Mb)
Thiomicrospira microaerophila ASL82 (3.1Mb)
Ca.Thioglobus singularis PS1 (1.71Mb)
Bathymodiolus azoricus symbiont BazSymA (1.86Mb)
Bathymodiolus thermophilus symbiont EPR9N (2.83Mb)
Bathymodiolus septemdierum symbiont Lau (2.37Mb)
Bathymodiolus septemdierum symbiont Myojin (1.47Mb)
uncultured SUP05 cluster bacterium (1.17Mb)
Ca. Thioglobus autotrophicus (1.51Mb)
Calyptogena okutanii symbiont (1.02Mb)
Calyptogena extenta symbiont (1.02Mb)
Calyptogena fausta symbiont (1.19Mb)
Calyptogena magnifica symbiont (1.16Mb)
Galathealinum brachiosum symbiont (3.77Mb)
Pseudoruegeria sabulilitoris GJMS35 (5.32Mb)
Pre-cambrian
2000
1500
1000
500
0
B
Abyssogena phaseoliformis
Calyptogena fausta
Calyptogena magnifica
Calyptogena extenta
Calyptogena marissinica
Corbicula fluminea
Dosinia altior
Macridiscus melanaegis
Ruditapes philippinarum
Dreissena polymorpha
Panopea abrupta
Venustaconcha ellipsiformis
Bathymodiolus japonicus
Bathymodiolus platifrons
Bathymodiolus childressi
Bathymodiolus securiformis
Bathymodiolus septemdierum
Modiolus modiolus
Modiolus philippinarum
Limnoperna fortunei
Mytilus coruscus
Mytilus galloprovincialis
Crassostrea gigas
Crassostrea virginica
Saccostrea glomerata
Pinctada martensii
Mizuhopecten yessoensis
Solemya elarraichensis
Solemya velum
Solemya pervernicosa
Solemya velesiana
Ascobulla fragilis
Onchidella celtica
Melibe leonina
Tritonia diomedea
Pre-cambrian
Paleozoic
Mesozoic
Cenozoic
600
500
400
300
200
100
0
divergence date (mya)